Received: 16 September 2024 | Accepted: 14 January 2025

DOI: 10.1111/head.14949

RESEARCH SUBMISSION

# Long-term evolution of white and gray matter structural properties in migraine

Álvaro Planchuelo-Gómez PhD[1] | Carmen Martín-Martín MSc[1] | Ángel L. Guerrero MD, PhD[2,3] | David García-Azorín MD, PhD[3,4] | Rodrigo de Luis-García PhD[1] | Santiago Aja-Fernández PhD[1]

[1]Image Processing Laboratory, Universidad de Valladolid, Valladolid, Spain

[2]Headache Unit, Department of Neurology, Hospital Clínico Universitario de Valladolid, Valladolid, Spain

[3]Department of Medicine, Universidad de Valladolid, Valladolid, Spain

[4]Department of Neurology, Hospital Universitario Río Hortega, Valladolid, Spain

**Correspondence**
David García-Azorín, Department of Medicine, Dermatology and Toxicology, University of Valladolid, Valladolid, 47011, Spain.
Email: dgazorin@ucm.es

**Funding information**
Ministerio de Ciencia y Tecnología, Grant/Award Number: PID2021-124407NB-I00 and TED2021-130758B-I00; Gerencia Regional de Salud CyL, Grant/Award Number: GRS 1727/A/18; Junta de Castilla y León, Grant/Award Number: VA156P24; European Social Fund Plus

## Abstract

**Objective:** To elucidate the specific brain changes linked to clinical diagnoses and distinct temporal progression in migraine.

**Background:** Gray (GM) and white matter (WM) differences were previously identified in chronic migraine (CM) compared to episodic migraine (EM). Regarding GM, patients with CM showed increased cortical thickness in the inferior temporal gyrus, and reduced surface area in the precuneus cortex, superior frontal and temporal gyri, and supramarginal gyrus. In the WM, widespread reduced axial and mean diffusivity have been observed in patients with CM in tracts such as the middle cerebellar peduncle, the internal capsule, the corticospinal tract, and the sagittal stratum. However, no longitudinal studies with a long follow-up have been conducted to comprehend how those differences evolve over an extended period, in relation to the clinical evolution of the disease.

**Methods:** A longitudinal study with a cohort design was conducted. Brain T1- and diffusion-weighted magnetic resonance imaging data were acquired in patients with migraine at two different timepoints, the first between May 2015 and July 2018, and the second between November 2021 and February 2022. Three WM descriptors and four GM morphometry parameters were extracted. Next, longitudinal changes were analyzed using generalized linear mixed models, after considering three different clinical groups: patients with a stable diagnosis (CM or EM) at both timepoints (24 CM, 31 EM), and 24 patients with CM who improved to EM.

**Results:** Different patterns of structural longitudinal changes were found depending on the clinical evolution. Regarding GM, patients with stable EM showed a longitudinal cortical thickness increase in the parietal and temporal cortex (annual relative change between 0.38% and 0.52% in five regions, adjusted $p$ between 0.013 and 0.017), and the postcentral gyrus (annual relative change of 0.37%, adjusted $p = 0.014$). Patients

**Abbreviations:** AD, axial diffusivity; ARC, annual relative coefficient; CC, cortical curvature; CM, chronic migraine; CTh, cortical thickness; DTI, diffusion tensor imaging; EM, episodic migraine; FA, fractional anisotropy; FMRIB, Oxford Centre for Functional MRI of the Brain; FSL, FMRIB Software Library; GM(V), gray matter (volume); ICHD-3, third edition of the International Classification of Headache Disorders; JHU WM, Johns Hopkins University International Consortium of Brain Mapping (ICBM)-DTI-81 White Matter Atlas; LC, longitudinal coefficient; MD, mean diffusivity; (d)MRI, (diffusion-weighted) magnetic resonance imaging; SA, surface area; $t_0$, baseline-time 0; $t_1$, longitudinal measurement-time 1; WM, white matter.

with stable CM and EM showed a longitudinal cortical thickness decrease in the posterior cingulate gyrus (annual relative change of 0.51%, adjusted $p = 0.027$, and 0.34%, adjusted-$p = 0.019$, respectively), and patients who improved from CM to EM showed no changes (corrected $p > 0.05$). Moreover, regarding WM, the patients with stable EM showed a longitudinal increase in fractional anisotropy in the cerebral peduncle (annual relative change of 0.24%, adjusted $p = 0.014$).

**Conclusion:** Differences in clinical evolution are linked to distinct patterns of structural changes, suggesting a heterogeneous impact of disease evolution on brain structure. Patients with CM who improved to EM showed no significant GM differences while those with longitudinally stable diagnoses showed cortical thickness maladaptation in pain processing-related regions and adaptation in other regions associated with migraine. Patients who improved from CM to EM showed an opposite longitudinal trend in large WM regions compared to stable patients, possibly as an adaptation to a distinct entity.

## Plain Language Summary

We do not know much about how the brain changes in patients who have migraine for many years, and understanding what changes occur may help to understand migraine progression and the effect of treatments. We examined changes in brain structure in patients with chronic and episodic migraine over 3 to 7 years and studied whether there are more or less changes in gray matter and white matter if a patient's condition improved from chronic to episodic migraine. We found that the brain of patients whose condition did not improve changed more over time than patients who showed improvement, and this might help to assign new therapies in these patients.

**KEYWORDS**
diffusion tensor imaging, gray matter, magnetic resonance imaging, migraine, white matter

## INTRODUCTION

Advances in migraine pathophysiology have highlighted the significance of biomarkers in the development of targeted treatments, although they have not been incorporated into routine clinical practice.[1] Among the numerous potential sources, such as blood, saliva, cerebrospinal fluid, neurophysiological signals, and imaging,[2] neuroimaging biomarkers are particularly valuable as they facilitate direct assessment of brain structure and function. In relation to migraine, these markers have revealed that patients with migraine exhibit distinctive structural and functional brain differences compared to healthy individuals.

Considering these results, this study used neuroimaging-based biomarkers to track changes in brain structure over time, aiming to provide valuable insights into migraine progression. Specifically, to study the structure of white (WM) and gray matter (GM) in patients with migraine, diffusion-weighted magnetic resonance imaging (dMRI) and morphometry parameters from T1-weighted MRI were employed, respectively. To date, cross-sectional MRI studies have identified structural WM and GM differences between patients with migraine and healthy controls, and in patients with episodic migraine (EM) with respect to chronic migraine (CM).[3,4] Regarding GM, patients with CM who had used no preventive treatment presented significant reduced surface area (SA) and increased cortical thickness (CTh), in multiple regions, compared to patients with EM.[5] Additionally, widespread WM regions showed reduced axial diffusivity (AD) and mean diffusivity (MD) in CM compared to EM.[6,7]

The precise nature of these abnormalities remains uncertain. Given the cross-sectional and case–control design of the existing studies, it is challenging to determine whether the findings are the cause or consequence of migraine. Recently, some studies have also begun to track these changes over time. In patients with EM, Liu et al.[8] observed that, after 1 year, there was a widespread reduction in GM volume (GMV), with no significant changes in the WM. Conversely, Messina et al.[9] reported that, after a follow-up period of >3 years, there was an increase in GMV in the frontoparietal regions, associated with a relatively higher headache frequency, and a decrease of GMV in the visual areas.

Despite these findings, no previous MRI studies have systematically analyzed the stable CM condition over time, the process of migraine chronification, or improvement from CM to EM. The annual incidence of transitioning from EM to CM is 2.5–3.1%, and it has been associated with factors such as ineffective or overuse of acute medication, obesity, depression, and stressful life events.[10,11]

Conversely, in the American Migraine Prevalence and Prevention study,[12] 26% of patients transitioned from CM to EM over a 2-year period. Additionally, in the Chronic Migraine Epidemiology and Outcomes study, 49.9% of patients transitioned to EM during a 3-month follow-up period.[13] Although CM has been linked to a higher susceptibility to migraine attacks, no biomarkers have been associated with the predisposition to migraine chronification or to the transition from CM to EM.

The objective of this study was to evaluate longitudinal MRI-based structural changes in WM and GM in patients with EM and CM, based on their clinical progression, with a particular focus on the improvement from CM to EM. We hypothesized that diffusion tensor imaging (DTI) and GM morphometry parameters may reveal distinct patterns of change among patients with stable diagnosis of EM and CM and those who have shown improvement from CM to EM.

## METHODS

### Study and sample characteristics

#### Study design

The present study was an observational analytic study with prospective cohort design. The local Ethics Committee of Hospital Clínico Universitario de Valladolid approved the study (PI: 14-197 and PI: 21-2449 for the first and second timepoints, respectively). Additionally, all participants read and signed a written consent form prior to their participation.

#### Study setting

The study was conducted in the headache unit of Hospital Clínico Universitario de Valladolid, a third level public university hospital covering 261,000 inhabitants. The recruitment period was between May 2015 and July 2018 (first recruitment). Patients were prospectively followed up for at least 3 years between November 2021 and February 2022 (last visit). Data were collected throughout the entire study period.

#### Participants

The study population consisted of adult patients with migraine, included if they: (i) were aged >18 years; (ii) had a confirmed diagnosis of migraine, according to the third edition of the International Classification of Headache Disorders (ICHD-3)[14]; (iii) agreed to participate. Patients were excluded if they: (i) were pregnant or breastfeeding; (ii) had any known neurological or psychiatric disorder different other than EM or CM, including anxiety and depression according to the medical history or the Hospital Anxiety and Depression Scale[15]; (iii) were under chronic treatment with any drug with potential effect on the central nervous system; (iv) were unable to describe their headache (e.g., cognitive disturbances); (v) were receiving or had received any drug with potential effect as migraine preventive drug at baseline before the first MRI acquisition; (vi) had a high-frequency EM at baseline, that is, 8–14 headache days/month in any of the preceding 3 months prior to the enrolment; (vii) onset of migraine after the age of 50 years; (viii) migraine onset shorter than 12 months; (ix) other chronic pain conditions. Patients with EM at baseline had no attacks with tension-type headache features. Patients with high-frequency EM were excluded at baseline to avoid any potential overlap with CM in the last months and the similarities with CM previously reported.[16,17] All patients were permitted to initiate migraine preventive treatment if prescribed in the first visit to the Headache Unit, after the first MRI acquisition.

The sample of this study at baseline originally comprised 58 patients with CM and 56 patients with EM that participated in previous studies.[5,7] Hence, the sample size of this study was based on the available data after follow-up, and the estimation of the sample size was conducted for the analysis at baseline.[5] MRI data were obtained in two different timepoints: baseline-time 0 ($t_0$) and longitudinal measurement-time 1 ($t_1$). The minimum time between measurements was 3 years. Patients were followed-up by in-person or telemedicine evaluations.

#### Variables

Patients' sex, age, years lived with migraine, time from onset of CM (months), number of headache and migraine days/month in the last month before the MRI acquisition, presence of medication overuse, and presence of aura were gathered. The clinical situation of patients over time was classified according to the ICHD-3 criteria.[14] The use of migraine preventive drugs after the first MRI acquisition, according to the Spanish national guidelines, was recorded.

All the patients received prescribed preventive treatment in accordance with the Spanish national guidelines for the treatment of migraine. The analysis aimed to evaluate the combined effect of all treatments used, rather than focusing on any specific drug. At the second timepoint, the initial diagnosis was preserved if there was unclear definition of the diagnosis according to the ICHD-3 criteria.

#### Data sources and measurements: MRI acquisition

Clinical data were obtained from electronic health records, by retrieving all clinical variables consistently by using structured questionnaires, interviews, and headache diaries. Patients were trained in the completion of headache diaries. The patients started to complete the headache diary at least 1 month before the first MRI acquisition and were requested to complete it through the whole follow-up. They included information about daily events related to headache, migraine, symptomatic treatment, and adverse effects. For this study, the diary was used to obtain information about the headache and migraine frequency, medication overuse, and aura.

The previous month to the second MRI acquisition, the patients were called to guarantee the accurate completion of the headache diary.

The MRI data were acquired in $t_0$ and $t_1$ at least 24 h after the last migraine attack and within 2 weeks after the clinical visit to the Headache Unit for both timepoints. This clinical visit refers to the first time that the patients were referred to the Headache Unit due to suspected migraine (first MRI acquisition), and the last follow-up visit before the MRI acquisition at the second timepoint. In each visit, the patients signed an informed consent to participate in the study. Further details about the first clinical visit can be found elsewhere.[7] Whole-brain high-resolution three-dimensional T1-weighted followed by dMRI were acquired using a Philips Achieva 3T MRI unit (Philips Healthcare, Best, The Netherlands) with a 32-channel head coil. The acquisition parameters were identical at both timepoints. The MRI data were checked by a neuroradiologist to identify potential structural abnormalities.

The acquisition of T1-weighted images was carried out using a Turbo Field Echo sequence with the following parameters: repetition time 8.1 ms, echo time 3.7 ms, flip angle 8°, 256 × 256 matrix size, spatial resolution $1 \times 1 \times 1\,mm^3$ and 160 sagittal slices covering the whole brain.

The acquisition parameters for dMRI were repetition time 9000 ms, echo time 86 ms, flip angle 90°, 61 diffusion gradient orientations, one baseline volume, *b*-value $1000\,s/mm^2$, 128 × 128 matrix size, spatial resolution $2 \times 2 \times 2\,mm^3$, and 66 axial slices.

All the images were acquired with a total acquisition time of 18 min in the MRI facility of the Universidad de Valladolid (Valladolid, Spain). The patients experienced no migraine attacks, at least in the previous 24 h to the MRI acquisition (both timepoints). The first MRI acquisition took place between May 2015 and July 2018, and the second between November 2021 and February 2022.

## Data analysis

### Processing of dMRI

Image preprocessing steps consisted of: (i) Marchenko–Pastur Principal Component Analysis denoising[18,19]; (ii) Gibbs ringing removal[20,21]; (iii) eddy currents and motion correction within each dMRI acquisition; and (iv) correction for B1 field inhomogeneity. MRtrix (version 3.0.2) was employed for these steps,[22] using *dwidenoise*, *mrdegibbs*, *dwifslpreproc*, and *dwibiascorrect*.[23–25] Further, a whole brain mask for each subject was obtained with *dwi2mask*.[26]

Three DTI metrics were calculated using *dtifit* from the Oxford Centre for Functional MRI of the Brain (FMRIB) Software Library (FSL, version 6.0)[27]: fractional anisotropy (FA), MD, and AD. The mean values of the three descriptors were obtained on 48 regions of interest from the Johns Hopkins University International Consortium of Brain Mapping (ICBM)-DTI-81 White Matter Atlas (JHU WM).[28] The maps of the descriptors were nonlinearly registered to the FMRIB-58 template in the Montreal Neurological Institute space with FSL using FMRIB's nonlinear image registration tool, using the FA as the map registered to the template, and applying the same transformation for the remaining descriptors. This process aligned all brains to the same position, independently of the different head positions between subjects and MRI acquisitions. Then, following the tract-based spatial statistics pipeline,[29] we generated a WM skeleton from the mean FA image and projected the diffusion measures onto the skeleton to obtain more robust measures. The average value of the metrics on the FA-skeleton inside each region of interest was calculated within the 2% and 98% percentiles.

### Parcellation and T1-weighted processing

The T1-weighted MRI data were processed to obtain morphometry parameters to assess GM structure. Automatic cortical parcellation was performed using the *recon-all* pipeline from *FreeSurfer* (version 6.0.0).[30–33] The automated parcellations were manually inspected to check the quality. For each subject, the results at both timepoints were adjusted with the "*-long*" option of the recon-all pipeline and four morphometry parameters were extracted from *FreeSurfer*: mean cortical curvature (CC), average CTh, GMV, and SA. The GMV was obtained for all the 84 GM regions from the Desikan–Killiany atlas,[34] while CC, CTh, and SA were calculated for the 68 cortical regions from the atlas. Additionally, the total intracranial volume was extracted.

## Statistical methods

The longitudinal analysis was based on generalized linear mixed models. In these models, the response or dependent variable was the average value of the assessed morphometry or diffusion parameter obtained from the analyzed subjects in a region from the Desikan–Killiany (GM) or the JHU WM Atlas (WM). The fixed effects, that is, the covariates, were the time in months between $t_0$ and $t_1$ acquisitions (longitudinal coefficient) and age, considering the time as the variable of interest and age as a confounding factor. In the GMV models, the total intracranial volume was included as an additional covariate (fixed effect). The considered random effect was the individual biological variability. The years lived with migraine was not included as a variable due to correlation with age. Three groups of patients were considered:

1. Longitudinal EM ($EM_0 \rightarrow EM_1$): 31 patients with EM at $t_0$ who stayed as EM at $t_1$.
2. Longitudinal CM ($CM_0 \rightarrow CM_1$): 24 patients with CM at $t_0$ who stayed as CM at $t_1$.
3. Improved CM ($CM_0 \rightarrow EM_1$): 24 patients with CM at $t_0$ who improved to EM at $t_1$.

For the first scenario, an additional assessment including only the patients who used at least one preventive treatment throughout

follow-up was carried out to evaluate potential effects related to the treatment.

Each of the three clinical groups were separately assessed to determine longitudinal changes within each group. The adjustment of three statistical models (one per clinical group) was equivalent to adjusting one model including the whole sample but assessing the interaction between the clinical group and the time between acquisitions in months. The reason for using a quantitative time variable instead of a categorical variable was accounting for the variability of the time between the two MRI acquisitions in the sample.

To correct for multiple comparisons, the Benjamini–Hochberg false discovery rate procedure was used for each set of comparisons.[35] The correction was applied to the coefficients assessing the effect of time (the longitudinal variable). To facilitate the interpretation of the coefficients, we calculated the relative change with respect to the baseline value, as follows:

$$\mathrm{ARC}\,(\%) = \frac{\mathrm{LC}}{x_0} \cdot 12 \cdot 100$$

where ARC is the annual relative coefficient, expressed in %, LC is the longitudinal coefficient associated with the time (change per month), and $x_0$ the mean of the considered metric in each region for the assessed group at baseline. The LC was estimated as the slope associated with the time in months between $t_0$ and $t_1$ (regressor) of the linear mixed model, being the MRI-based parameter the scalar response.

To evaluate the differences in clinical and demographic characteristics between the three groups, we assessed the normality and homogeneity of variance of quantitative continuous variables using the Shapiro–Wilk and Levene's tests, respectively. For non-normal and unequal variances cases, the Kruskal–Wallis test was applied, using the Conover–Iman post hoc test for pairwise comparisons. If the assumptions were met, we used analysis of variance followed by Tukey–Kramer post hoc tests. Categorical variables were analyzed using the chi-squared test, with Fisher's exact test employed for pairwise comparisons. The diagnosis of the generalized linear mixed models was conducted with Pearson's residuals, checking the independence of errors and variance homoscedasticity comparing them with the predicted values from the model. The normality of the residuals was checked with Q–Q plots and density plots. The relationship between the MRI-based parameter and the time between MRI measurements was checked with scatter plots. If the assumptions of the model were not met, the results were not considered as statistically significant.

All hypothesis tests were two-tailed and considered significant at a $p < 0.05$. R statistical software (version 4.1.2) was employed to carry out the whole statistical analysis.[36]

## RESULTS

The final sample comprised 81 patients: 48 with CM and 33 with EM in $t_0$. In all, 10 patients with CM and 23 with EM were excluded due to clinical conditions (e.g., pregnancy), MRI contraindications (e.g., claustrophobia), and non-clinical or MRI-unrelated reasons (e.g., moving to another town). The specific number of excluded subjects for each reason is shown in Table S1. The three assessed groups were distributed as follows: 31 patients with $EM_0 \rightarrow EM_1$, 24 patients with $CM_0 \rightarrow CM_1$, and 24 patients with $CM_0 \rightarrow EM_1$. Two additional patients with EM at $t_0$ were discarded because they had a diagnosis of CM at $t_1$, as this number of patients was excessively low to conduct any assessment, and to avoid any bias associated with a higher heterogeneity in the $EM_0 \rightarrow EM_1$ group. Figure 1 shows a scheme of the distribution of patients at $t_0$ and $t_1$ times, including all the patients who were initially recruited. A complete-case analysis was conducted, including the 79 patients from the three mentioned groups, and the data from the two excluded subjects or the patients

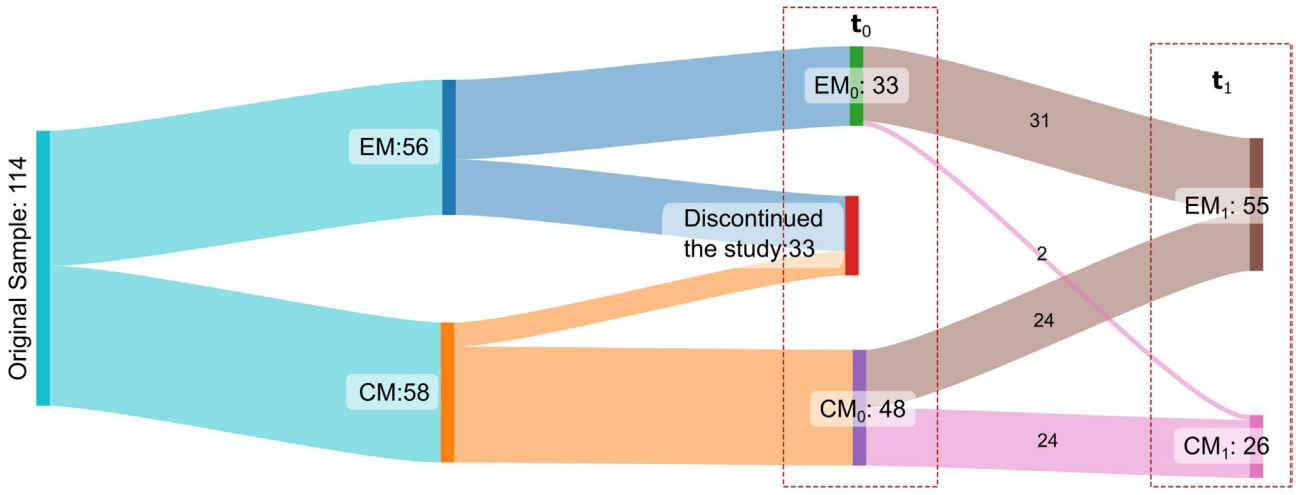


**FIGURE 1** Sankey's diagram of the patients with migraine within two different acquisition times. The patients included in the final sample without missing data were the 31 patients with episodic migraine (EM) at $t_0$ and $t_1$, the 24 patients with chronic migraine (CM) at $t_0$ and EM at $t_1$, and the 24 patients with CM at $t_0$ and $t_1$. The 33 patients who discontinued the study and the two patients with EM at $t_0$ and CM at $t_1$ were excluded, as a complete case analysis was conducted.

with only one MRI acquisition were not used. There were no missing data in these 79 patients. The mean time between both acquisitions was >60 months for the three groups (range 40–79 months), without statistically significant differences between the groups (Table 1). The median (interquartile range) number of preventive treatments after the first MRI acquisition was 1 (0–2) for the $EM_0 \rightarrow EM_1$ group, 2 (1–2) for the $CM_0 \rightarrow EM_1$ group, and 2 (1–3.3) $CM_0 \rightarrow CM_1$ group (Table 1). All patients with an initial CM diagnosis and 18 out of 31 patients with an initial EM diagnosis (58%) were using a preventive treatment at the time of the second MRI acquisition. The number of patients

**TABLE 1** Clinical and demographic characteristics of the three assessed groups of patients with migraine at both timepoints.

| **First timepoint ($t_0$)** | **$EM_0 \rightarrow EM_1$ ($t_0$)** | **$CM_0 \rightarrow EM_1$ ($t_0$)** | **$CM_0 \rightarrow CM_1$ ($t_0$)** | **Statistical test** |
|---|---|---|---|---|
| Sex, male/female, *n* (%) | 6/25 (19/81) | 4/20 (17/83) | 0/24 (0/100) | [a] $\chi^2(2) = 5.08$, $p = 0.079$ |
| Age, years, mean (SD) | 37.9 (8.3) | 39.3 (8.7) | 36.8 (8.0) | [b] $F(2,76) = 0.51$, $p = 0.603$ |
| Years lived with migraine, median (IQR) | 11 (4.5–21) | 18.5 (12.5–26.3) | 18.5 (13.3–22.3) | [c] $\chi^2(2) = 5.66$, $p = 0.059$ |
| Time from onset of chronic migraine, months, median (IQR) | NA | 8 (5.5–24) | 12 (6–25.5) | [d] $U = 331.50$, $p = 0.372$ |
| Headache frequency, days/month, median (IQR) | 3 (2–5) | 25 (20–25) | 25 (20–30) | [c] $\chi^2(2) = 53.67$, $p < 0.001$<br>G1–G2: $p < 0.001$<br>G1–G3: $p < 0.001$ |
| Migraine frequency, days/month, median (IQR) | 3 (2–5) | 13.5 (9.75–20) | 10 (9.8–16.3) | [c] $\chi^2(2) = 48.80$, $p < 0.001$<br>G1–G2: $p < 0.001$<br>G1–G3: $p < 0.001$ |
| Medication overuse, *n* (%) | 0 (0) | 19 (79) | 17 (71) | [a] $\chi^2(2) = 43.05$, $p < 0.001$<br>G1–G2: $p < 0.001$<br>G1–G3: $p < 0.001$ |
| Aura, *n* (%) | 5 (16) | 0 (0) | 1 (4) | [a] $\chi^2(2) = 5.59$, $p = 0.061$ |
| **Second timepoint ($t_1$)** | **$EM_0 \rightarrow EM_1$ ($t_1$)** | **$CM_0 \rightarrow EM_1$ ($t_1$)** | **$CM_0 \rightarrow CM_1$ ($t_1$)** | **Statistical test** |
| Sex, male/female, *n* (%) | 6/25 (19/81) | 4/20 (17/83) | 0/24 (0/100) | [a] $\chi^2(2) = 5.08$, $p = 0.079$ |
| Age, years, mean (SD) | 43.1 (8.2) | 44.5 (8.7) | 42.1 (8.1) | [b] $F(2,76) = 0.49$, $p = 0.614$ |
| Years lived with migraine, median (IQR) | 15 (8.5–26) | 22.5 (16.5–30.5) | 23.5 (18.8–28) | [c] $\chi^2(2) = 5.38$, $p = 0.068$ |
| Time from onset of chronic migraine, months, median (IQR) | NA | NA | 82 (68–88) | NA |
| Headache frequency, days/month, median (IQR) | 4 (2–7) | 6.5 (4.8–10) | 20 (18.8–30) | [a] $\chi^2(2) = 52.57$, $p < 0.001$<br>G1–G2: $p = 0.001$<br>G1–G3: $p < 0.001$<br>G2–G3: $p < 0.001$ |
| Migraine frequency, days/month, median (IQR) | 2 (0–3) | 2 (0–3) | 6.5 (4–10) | [c] $\chi^2(2) = 26.42$, $p < 0.001$<br>G1–G3: $p < 0.001$<br>G2–G3: $p < 0.001$ |
| Medication overuse, *n* (%) | 3 (10) | 8 (33) | 16 (67) | [a] $\chi^2(2) = 19.54$, $p < 0.001$<br>G1–G2: $p = 0.043$<br>G1–G3: $p < 0.001$<br>G2–G3: $p = 0.042$ |
| Aura, *n* (%) | 4 (13) | 6 (25) | 6 (25) | [a] $\chi^2(2) = 1.71$, $p = 0.426$ |
| Number of preventive treatments, median (IQR) | 1 (0–2) | 2 (1–2) | 2 (1–3.3) | [c] $\chi^2(2) = 10.26$, $p = 0.006$<br>G1–G2: $p = 0.005$<br>G1–G3: $p = 0.002$ |
| Time between MRI acquisitions, months, mean (SD) | 62.5 (8.6) | 61.6 (10.6) | 61.7 (8.3) | [b] $F(2,76) = 0.10$, $p = 0.909$ |

Abbreviations: $CM_0$, chronic migraine at baseline-time 0; $CM_1$, chronic migraine at longitudinal measurement-time 1; $EM_0$, episodic migraine at baseline-time 0; $EM_1$, episodic migraine at longitudinal measurement-time 1; G1, $EM_0 \rightarrow EM_1$; G2, $CM_0 \rightarrow EM_1$; G3, $CM_0 \rightarrow CM_1$; IQR, interquartile range; NA, not available; SD, standard deviation.

[a]Chi-squared test and *p* values of Fisher's tests.

[b]Analysis of variance.

[c]Kruskal–Wallis test and *p* values for Conover–Iman post hoc test.

[d]Mann–Whitney *U* test.

with medication overuse was higher in the second timepoint for the stable EM group, and lower for the two groups of patients with CM (Table 1).

Table 1 shows the detailed demographic and clinical features of the three groups of patients at $t_0$ and $t_1$. No statistically significant age or sex differences were found at both timepoints. Considering all the patients with CM as a single group, they showed significantly higher value of years lived with migraine (at $t_0$; $U=518$, $p=0.023$). However, these differences were not identified when separating the patients with CM into two groups. Patients with CM, considering the two groups, showed significantly higher value of frequency of headache (at $t_0$ and $t_1$), migraine attacks (at $t_0$ and $t_1$), and medication overuse (at $t_0$ and $t_1$).

For the following sections, an additional analysis adjusting the results for sex was performed. For GM and WM, the results were similar in relation to the regions with uncorrected significant results, and the corrected results had no variations. Therefore, as the $CM_0 \rightarrow CM_1$ group had only women, the results for the common analysis for all groups, without correcting for sex, are reported.

## Longitudinal analysis: Gray matter

The ARCs after the adjustment for age effects and the correction for multiple comparisons ($0.001 < \text{adjusted } p < 0.038$) are shown in Table 2. Statistically significant longitudinal changes were found only in those groups presenting stable condition: $EM_0 \rightarrow EM_1$ (CC and CTh) and $CM_0 \rightarrow CM_1$ (CTh and GMV), while no statistically significant longitudinal changes were observed in any region for the $CM_0 \rightarrow EM_1$ group.

In the $EM_0 \rightarrow EM_1$ group, a statistically significant increase in curvature was observed in the temporal pole, an increase in thickness was found in six regions from the temporal cortex, the inferior parietal cortex and the postcentral gyrus, and a decrease in thickness was identified in the posterior cingulate gyrus. These changes were found in the left hemisphere for all cases. The significant thickness reduction in the left posterior cingulate gyrus was also observed in the $CM_0 \rightarrow CM_1$ group, this being the only common longitudinal change in GM morphology for the three assessed groups. In addition, for the $CM_0 \rightarrow CM_1$ group, significant thickness and volume reduction was detected in the right posterior cingulate gyrus and left

**TABLE 2** The annual relative coefficient of the statistically significant (corrected $p < 0.05$) variations of the gray matter morphometry parameters based on the longitudinal coefficient of the complete generalized linear mixed model. Regions of interest defined by the Desikan–Killiany atlas.

| | $EM_0 \rightarrow EM_1$ | | | $CM_0 \rightarrow EM_1$ | | | $CM_0 \rightarrow CM_1$ | | |
|---|---|---|---|---|---|---|---|---|---|
| **ROI** | **CC** | **CTh** | **GMV** | **CC** | **CTh** | **GMV** | **CC** | **CTh** | **GMV** |
| L. BSTS | | 0.42<br>$p=0.014$ | | | | | | | |
| L. IPC | | 0.38<br>$p=0.014$ | | | | | | | |
| L. ITG | | 0.52<br>$p=0.014$ | | | | | | | |
| L. MTG | | 0.43<br>$p=0.017$ | | | | | | | |
| L.PG | | 0.37<br>$p=0.014$ | | | | | | | |
| L. PCG | | −0.34<br>$p=0.019$ | | | | | | −0.51<br>$p=0.028$ | |
| L. SPC | | 0.41<br>$p=0.014$ | | | | | | | |
| L. TP | 1.19<br>$p=0.001$ | | | | | | | | |
| R. PCG | | | | | | | | −0.50<br>$p=0.038$ | |
| L. HI | | | | | | | | | −0.71<br>$p=0.010$ |

*Note*: All $p$ values are corrected. Green boxes denote positive association, while red boxes indicate negative association.

Abbreviations: BSTS, banks of the superior temporal sulcus; CC, cortical curvature; $CM_0$, chronic migraine at baseline-time 0; $CM_1$, chronic migraine at longitudinal measurement-time 1; CTh, cortical thickness; $EM_0$, episodic migraine at baseline-time 0; $EM_1$, episodic migraine at longitudinal measurement-time 1; GMV, gray matter volume; HI, hippocampus; IPC, inferior parietal cortex; ITG, inferior temporal gyrus; L., Left; MTG, middle temporal gyrus; PCG, posterior cingulate gyrus; PG, postcentral gyrus; R., right; ROI, region of interest; SPC, superior parietal cortex; TP, temporal pole.

hippocampus, respectively. The coefficients associated with age for the same regions, the total variation combining longitudinal and age effects, and the mean values of the regions at both timepoints are shown in Table S2.

Tables 3 and 4 show the uncorrected significant results of the ARC after adjusting for aging across the three groups. Although corrections for multiple comparisons were not applied, these results are still of interest as to show trends that could be substantiated in future works with larger sample size. Details on annual changes and other results are given in Tables S3–S5.

For the $EM_0 \rightarrow EM_1$ group, after excluding the patients who used no preventive treatments, statistically significant longitudinal changes were found in the same plus additional regions compared to the analysis with the whole group ($0.008 < \text{corrected } p < 0.049$). Curvature increase was observed in the temporal pole, pericalcarine cortex and insula, and thickness increase was found in eight regions from the temporal cortex, the inferior parietal cortex and the postcentral and paracentral gyri. The corrected and uncorrected results are shown in Table S6.

### Longitudinal analysis: White matter

Table 5 shows the ARCs for the diffusion descriptors in WM after the adjustment for age and the corrections for multiple comparisons (adjusted $p = 0.016$). The only statistically significant result was a longitudinal FA increase in the left cerebral peduncle for the patients in the $EM_0 \rightarrow EM_1$ group. The coefficients associated with age for this case, the total variation combining longitudinal and age effects, and the mean values at both timepoints are shown in Table S7.

Table 6 presents the uncorrected results across the three groups, adjusted for age but not for multiple comparisons. Regarding the uncorrected results, no significant longitudinal changes in MD were found for any group. For the $CM_0 \rightarrow CM_1$ group, FA increased in five regions. No significant longitudinal changes were observed for AD or MD. In the $CM_0 \rightarrow CM_1$ group, FA increased in the corticospinal tract but decreased in four other regions. Patients in the $EM_0 \rightarrow EM_1$ group showed FA increases in three additional regions, and a decrease in the uncinate fasciculus. AD increased in three regions. Stable groups ($CM_0 \rightarrow CM_1$ and $EM_0 \rightarrow EM_1$) shared significant FA increases in both cerebral peduncles, consistently with corrected results. Detailed results are in Table S8.

For the $EM_0 \rightarrow EM_1$ group, after excluding the patients who used no preventive treatments, results were similar compared to the analysis with the whole group, and statistically significant changes (corrected $p = 0.014$) were found. An FA increase was observed in the right cerebral peduncle and posterior limb of the internal capsule, and an FA decrease was found in the left uncinate fasciculus. The corrected and uncorrected results are shown in Table S6.

## DISCUSSION

This work aimed to unravel the structural longitudinal changes in the brain of patients with migraine over time. We characterized structural GM and WM changes over a span of at least 3 years, which is significantly longer than the duration examined in previous studies. Our research focused on three distinct migraine evolution scenarios: stable EM; stable CM; and CM improving to EM. To elucidate the relationship between migraine evolution and brain structure, we utilized morphometric and DTI parameters.

Age-corrected longitudinal changes revealed significant structural changes over time, particularly in GM morphology, with less pronounced but still noticeable diffusion changes in WM. The progression of migraine across different diagnostic stages is associated with distinct patterns of change, suggesting that the impact of disease evolution on brain structure is heterogeneous and may be influenced by the specific nature and course of the condition.

The GM and WM showed different patterns. In GM, distinct changes emerged in the progression of stable EM and stable CM across several regions, while in WM, changes appeared in the right cerebral peduncle. This discrepancy in the number of affected areas, specific regions and metrics provides insights into the underlying evolution of brain structure, suggesting that GM and WM respond differently to the progression of migraine.

In terms of the GM evolution, the three groups displayed distinct patterns. The group transitioning from CM to EM showed no significant longitudinal changes in any region, while the other two groups did. Specifically, the stable EM group demonstrated a predominant increase in thickness. In contrast, the stable CM group exhibited a decrease in thickness in the bilateral posterior cingulate gyrus and a reduction in hippocampal volume.

The left posterior cingulate gyrus is the only region showing similar behavior across groups, precisely in those with stable diagnoses, experiencing a decrease in thickness—0.34% annually for EM and 0.51% for CM. This region showed no change in the $CM_0 \rightarrow EM_1$ group, even in uncorrected data, indicating differentiated structural behavior linked to diagnostic improvement. The posterior cingulate gyrus has been linked to pain processing and perception in various pathologies. It is a key component of the default mode network involved in conscious processing of pain and reappraisal of pain perception.[37] Abnormal connectivity in this region is linked to increased pain sensitivity and abnormal pain processing in individuals with migraine.[38] Similarly, patients with chronic pain showed decreased activity in this region,[39] which correlates with higher pain intensities. Interestingly, another study presented findings that contrast with ours[40]; their analysis found that migraine improvement was associated with a decrease of thickness in this area. These discrepancies may be attributed to the lack of appropriate statistical corrections in their study.

The $CM_0 \rightarrow CM_1$ group exhibited a decrease in volume in the left hippocampus, a pattern not observed in the other groups, except for uncorrected results in the $EM_0 \rightarrow EM_1$ group, which showed a

**TABLE 3** The annual relative coefficient of the statistically significant (uncorrected $p < 0.05$) variations of the gray matter morphometry parameters based on the longitudinal coefficient of the complete generalized linear mixed model. Regions of interest were defined by the Desikan–Killiany atlas.

| | $EM_0 \rightarrow EM_1$ | | | | $CM_0 \rightarrow EM_1$ | | | | $CM_0 \rightarrow CM_1$ | | | |
|---|---|---|---|---|---|---|---|---|---|---|---|---|
| **ROI** | **CC** | **CTh** | **SA** | **GMV** | **CC** | **CTh** | **SA** | **GMV** | **CC** | **CTh** | **SA** | **GMV** |
| L. BSTS | | **0.42** | | | | 0.39 | | | | | | |
| L. CACG | | −0.37 | | −1.16 | | | | | | | | |
| L. CMFG | | | | −0.74 | | | | | | | | |
| L. CUN | | 0.40 | | | | 0.48 | | | | | | |
| L. IPC | | **0.38** | | | | 0.51 | | | | | | |
| L. ITG | | **0.52** | | | 0.46 | | | | 0.34 | | | |
| L. LOC | | 0.28 | | | | | | | | | | |
| L. LOFG | | | | | | | | | | | 0.60 | |
| L. LG | | | | | | | | | | −0.47 | | |
| L. MTG | 0.30 | **0.43** | | | | 0.42 | | | | | | |
| L. PaG | | 0.34 | | | | 0.66 | −0.81 | | | | | |
| L. POr | | | | | | | −0.87 | | | | | |
| L. PT | | | 0.60 | | | | | | | | | |
| L. PCC | 0.50 | | | | | | | | | | | |
| L. PG | | **0.37** | | | | 0.47 | −0.55 | | | | | |
| L. PCG | | **−0.34** | | | | | | | | **−0.51** | | −0.91 |
| L. PrG | | | | | | | −0.72 | | | | | |
| L. RACG | | | | | | | | | 0.64 | | | |
| L. SPC | | **0.41** | | | | 0.57 | | | | | | |
| L. SPG | | 0.26 | | | | 0.29 | | | | | | |
| L. FP | | | | −0.82 | | | | | | | | |
| L. TP | **1.19** | | | | | | | | | | | |
| L. INS | 0.40 | | 0.62 | | | | | | | | | |
| R. CACG | | | | | | | | | 0.51 | | −1.20 | −1.23 |
| R. EC | | | | | | | | | | | | −1.07 |
| R. ITG | | 0.42 | | | | | | | | | | |
| R. IPC | | | | | | | | | | | | −0.72 |
| R. LOFG | | | 0.68 | | | | | | | | 0.75 | |
| R. LG | | | | | | | | | | −0.36 | | |
| R. PaG | | 0.44 | | | | 0.55 | −1.11 | | | | | |
| R. POp | | | 0.75 | | | | | | | | | |
| R.POr | | | 0.47 | | | | | | | | | |
| R. PT | | | | | | | | | | −0.41 | | |
| R. PCC | 0.53 | | | | | 0.72 | | | | | | |
| R. PG | | 0.35 | | | | 0.50 | | | | | | |
| R. PCG | | | | | | | | | | **−0.50** | | −1.00 |
| R. PrG | | | | | | | −0.67 | | | | | −0.50 |
| R. RACG | | | | | | 0.50 | | | | | | |
| R. RMFG | | | | −0.67 | | | | | | | | |
| R. SPC | | 0.35 | | | | 0.38 | | | | | | |
| R. FP | | | | | | | | | | −0.49 | | |
| R. TP | | | | | | | | | | −0.51 | | −0.73 |

(Continues)

TABLE 3 (Continued)

| | $EM_0 \rightarrow EM_1$ | | | | $CM_0 \rightarrow EM_1$ | | | | $CM_0 \rightarrow CM_1$ | | | |
|---|---|---|---|---|---|---|---|---|---|---|---|---|
| ROI | CC | CTh | SA | GMV | CC | CTh | SA | GMV | CC | CTh | SA | GMV |
| R. TTG | | | | | | 0.55 | | | | | | |
| R. INS | | | 0.56 | | | | | | | | | |
| L. PAL | | | | | | | | | | | | −0.56 |
| L. HI | | | | −0.39 | | | | | | | | **−0.71** |
| R. CER | | | | | | | | −0.46 | | | | −0.48 |
| R. PUT | | | | | | | | | | | | −0.55 |
| R. HIP | | | | | | | | | | | | −0.54 |
| R. ACC | | | | | | | | | | | | −0.80 |

*Note*: Cells with numeric values in bold represent adjusted $p < 0.05$.

Abbreviations: ACC, accumbens; BSTS, banks of the superior temporal sulcus; CACG, caudal anterior cingulate gyrus; CC, cortical curvature; CER, cerebellum; $CM_0$, chronic migraine at baseline-time 0; $CM_1$ chronic migraine at longitudinal measurement-time 1; CMFG, caudal middle frontal gyrus; CTh, cortical thickness; CUN, cuneus; EC, entorhinal cortex; $EM_0$, episodic migraine at baseline-time 0; $EM_1$, episodic migraine at longitudinal measurement-time 1; FP, frontal pole; GMV, gray matter volume; HI, hippocampus; INS, insula; IPC, inferior parietal cortex; ITG, inferior temporal gyrus; L., Left; LG, lingual gyrus; LOC, lateral occipital cortex; LOFG, lateral orbitofrontal gyrus; MTG, middle temporal gyrus; PaG, paracentral gyrus; PAL, pallidum; PCC, pericalcarine cortex; PCG, posterior cingulate gyrus; PG, postcentral gyrus; POp, pars opercularis; POr, pars orbitalis; PrG, precentral gyrus; PT, pars triangularis; PUT, putamen; R., right; RACG, rostral anterior cingulate gyrus; RMFG, rostral middle frontal gyrus; ROI, region of interest; SA, surface area; SPC, superior parietal cortex; SPG, supramarginal gyrus; TP, temporal pole; TTG, transverse temporal gyrus.

similar trend to that of the posterior cingulate gyrus. The hippocampus is involved in pain processing, attention, and stress response, and it plays a significant role in the evolution of migraine. A 1-year follow-up study found a decrease in volume in this region in patients with newly diagnosed EM[8] and identified maladaptive changes associated with high headache frequency.[41] The changes in these two regions within the stable groups may indicate (mal)adaptation to a "stable" pain perception over time.

Other GM regions that showed significant longitudinal changes included the left inferior and middle temporal gyri, inferior parietal cortex, temporal pole, and precuneus. Although these areas are less prominent in pain processing, they have been shown to play significant roles in migraine. For instance, the inferior temporal gyrus presented reduced thickness in both CM and EM compared to healthy controls.[5] Additionally, the inferior parietal cortex thickness correlated positively with pain thresholds in migraine.[42] Furthermore, thickness in the middle temporal gyrus and temporal pole were able to distinguish those with migraine from healthy controls.[43] Changes in functional connectivity in the thalamus, particularly with the precuneus, have been observed in patients with migraine.[44,45]

Regarding the WM analysis, only one region exhibited significant longitudinal changes: the right cerebral peduncle in the stable EM group. This region, involved in motor control, sensory relay, and pain processing, also exhibited additional anisotropy changes in the bilateral cerebral peduncles in the uncorrected results. However, these changes were observed only in the stable migraine groups, not in $CM_0 \rightarrow EM_1$. Prior research on chronic musculoskeletal pain,[46] neuropathic pain,[47] and trigeminal neuralgia[48] has suggested the possible involvement of the cerebral peduncle in pain processing. Notably, among the patients in the stable EM group who utilized at least one preventive treatment, additional significant changes were observed, suggesting the possible influence of the preventive treatment on WM structures.

A glimpse at the uncorrected results (Table 6) may provide further insights into WM behavior. In the $CM_0 \rightarrow EM_1$ group, a reduction in anisotropy was observed in the bilateral anterior limb of the internal capsule. In the stable EM group, changes in FA and AD were evident in the posterior limb of the internal capsule, a region that exhibited statistically significant FA changes in the patients who used preventive treatments. These regions appear to be sensitive to migraine-related alterations, as supported by previous cross-sectional studies[6,7] and other pain conditions like chronic musculoskeletal pain,[46] trigeminal neuralgia,[48] migraine without aura,[49] and persistent headache associated with coronavirus disease 2019.[50] These results may reflect a clue about the potential of disease-modification of preventive medications, driving WM changes in patients who use them and improve from a CM frequency towards an EM situation. While MD is typically an important marker in cross-sectional migraine studies, no longitudinal changes were observed, even for the uncorrected data. Conversely, the patients with stable EM exhibited increased AD.

Overall, fewer regions exhibited significant longitudinal changes in WM compared to GM, and the rates of change were much lower, suggesting that GM is more susceptible to disruption. Based on the results, it can be hypothesized that stable and unstable clinical conditions lead to opposite changes in WM. These changes may be related to adaptive and maladaptive neuroplasticity, respectively, suggesting an imbalance in how the brain responds to different migraine states. However, when considering corrected data, the changes in WM do not accurately reflect the evolution of the patients' conditions.

The changes observed in regions associated with central pain processing differ from those in other areas related to the migraine

**TABLE 4** Uncorrected *p* values of the statistically significant (uncorrected $p < 0.05$) variations of the gray matter morphometry parameters based on the longitudinal coefficient the complete generalized linear mixed model. Regions of interest were defined by the Desikan–Killiany atlas.

| | $EM_0 \rightarrow EM_1$ | | | | $CM_0 \rightarrow EM_1$ | | | | $CM_0 \rightarrow CM_1$ | | | |
|---|---|---|---|---|---|---|---|---|---|---|---|---|
| **ROI** | **CC** | **CTh** | **SA** | **GMV** | **CC** | **CTh** | **SA** | **GMV** | **CC** | **CTh** | **SA** | **GMV** |
| L. BSTS | | **0.002** | | | | 0.009 | | | | | | |
| L. CACG | | 0.031 | | 0.040 | | | | | | | | |
| L. CMFG | | | | 0.042 | | | | | | | | |
| L. CUN | | 0.043 | | | | 0.025 | | | | | | |
| L. IPC | | **0.002** | | | | 0.014 | | | | | | |
| L. ITG | | **0.001** | | | 0.029 | | | | 0.031 | | | |
| L. LOC | | 0.033 | | | | | | | | | | |
| L. LOFG | | | | | | | | | | | 0.033 | |
| L. LG | | | | | | | | | | 0.017 | | |
| L. MTG | 0.026 | **0.003** | | | | 0.029 | | | | | | |
| L. PaG | | 0.018 | | | | 0.004 | 0.038 | | | | | |
| L. POr | | | | | | | 0.038 | | | | | |
| L. PT | | | 0.046 | | | | | | | | | |
| L. PCC | 0.012 | | | | | | | | | | | |
| L. PG | | **0.002** | | | | 0.032 | 0.013 | | | | | |
| L. PCG | | **0.004** | | | | | | | | **<0.001** | | 0.012 |
| L. PrG | | | | | | | 0.016 | | | | | |
| L. RACG | | | | | | | | | 0.013 | | | |
| L. SPC | | **0.001** | | | | 0.006 | | | | | | |
| L. SPG | | 0.028 | | | | 0.042 | | | | | | |
| L. FP | | | | 0.008 | | | | | | | | |
| L. TP | **<0.001** | | | | | | | | | | | |
| L. INS | 0.013 | | 0.008 | | | | | | | | | |
| R. CACG | | | | | | | | | 0.028 | | 0.006 | 0.012 |
| R. EC | | | | | | | | | | | | 0.032 |
| R. ITG | | 0.012 | | | | | | | | | | |
| R. IPC | | | | | | | | | | | | 0.012 |
| R. LOFG | | | 0.004 | | | | | | | | 0.037 | |
| R. LG | | | | | | | | | | 0.035 | | |
| R. PaG | | 0.010 | | | | 0.002 | 0.002 | | | | | |
| R. POp | | | 0.003 | | | | | | | | | |
| R. POr | | | 0.047 | | | | | | | | | |
| R. PT | | | | | | | | | | 0.022 | | |
| R. PCC | 0.006 | | | | | 0.039 | | | | | | |
| R. PG | | 0.007 | | | | 0.003 | | | | | | |
| R. PCG | | | | | | | | | | **0.001** | | 0.009 |
| R. PrG | | | | | | | 0.034 | | | | | 0.036 |
| R. RACG | | | | | | 0.018 | | | | | | |
| R. RMFG | | | | 0.031 | | | | | | | | |
| R. SPC | | 0.011 | | | | 0.028 | | | | | | |
| R. FP | | | | | | | | | | 0.031 | | |
| R. TP | | | | | | | | | | 0.016 | | 0.026 |

(Continues)

**TABLE 4** (Continued)

| | $EM_0 \rightarrow EM_1$ | | | | $CM_0 \rightarrow EM_1$ | | | | $CM_0 \rightarrow CM_1$ | | | |
|---|---|---|---|---|---|---|---|---|---|---|---|---|
| **ROI** | **CC** | **CTh** | **SA** | **GMV** | **CC** | **CTh** | **SA** | **GMV** | **CC** | **CTh** | **SA** | **GMV** |
| R. TTG | | | | | | 0.008 | | | | | | |
| R. INS | | | 0.033 | | | | | | | | | |
| L. PAL | | | | | | | | | | | | 0.025 |
| L. HI | | | | 0.044 | | | | | | | | **0.001** |
| R. CER | | | | | | | | 0.014 | | | | 0.035 |
| R. PUT | | | | | | | | | | | | 0.039 |
| R. HIP | | | | | | | | | | | | 0.015 |
| R. ACC | | | | | | | | | | | | 0.035 |

*Note*: Cells with numeric values in bold represent adjusted $p < 0.05$.

Abbreviations: ACC, accumbens; BSTS, banks of the superior temporal sulcus; CACG, caudal anterior cingulate gyrus; CC, cortical curvature; CER, cerebellum; $CM_0$, chronic migraine at baseline-time 0; $CM_1$, chronic migraine at longitudinal measurement-time 1; CMFG, caudal middle frontal gyrus; CTh, cortical thickness; CUN, cuneus; EC, entorhinal cortex; $EM_0$, episodic migraine at baseline-time 0; $EM_1$, episodic migraine at longitudinal measurement-time 1; FP, frontal pole; GMV, gray matter volume; HI, hippocampus; INS, insula; IPC, inferior parietal cortex; ITG, inferior temporal gyrus; L., Left; LG, lingual gyrus; LOC, lateral occipital cortex; LOFG, lateral orbitofrontal gyrus; MTG, middle temporal gyrus; PaG, paracentral gyrus; PAL, pallidum; PCC, pericalcarine cortex; PCG, posterior cingulate gyrus; PG, postcentral gyrus; POp, pars opercularis; POr, pars orbitalis; PrG, precentral gyrus; PT, pars triangularis; PUT, putamen; R., right; RACG, rostral anterior cingulate gyrus; RMFG, rostral middle frontal gyrus; ROI, region of interest; SA, surface area; SPC, superior parietal cortex; SPG, supramarginal gyrus; TP, temporal pole; TTG, transverse temporal gyrus.

**TABLE 5** The annual relative coefficient of the statistically significant (false discovery rate corrected $p < 0.05$) variations of the diffusion descriptors in white matter based on the longitudinal coefficient of the complete generalized linear mixed model. Regions of interest were defined by the Johns Hopkins University ICBM-DTI-81 White Matter Atlas.

| | $EM_0 \rightarrow EM_1$ | | | $CM_0 \rightarrow EM_1$ | | | $CM_0 \rightarrow CM_1$ | | |
|---|---|---|---|---|---|---|---|---|---|
| **ROI** | **FA, %** | **AD, %** | **MD, %** | **FA, %** | **AD, %** | **MD, %** | **FA, %** | **AD, %** | **MD, %** |
| R. CP | 0.24<br>$p = 0.016$ | | | | | | | | |

*Note*: The *p* value is corrected.

Abbreviations: AD, axial diffusivity; $CM_0$, chronic migraine at baseline-time 0; $CM_1$, chronic migraine at longitudinal measurement-time 1; CP, cerebral peduncle; $EM_0$, episodic migraine at baseline-time 0; $EM_1$, episodic migraine at longitudinal measurement-time 1; FA, fractional anisotropy; MD, mean diffusivity; R., right; ROI, region of interest.

experience that are not directly involved in pain processing. Maladaptive changes, which were particularly evident in individuals with "stable" CM, contrast with adaptative changes seen in those with "stable" EM. Both types of changes exhibit similar longitudinal characteristics in response to migraine over time. A detailed examination of the results revealed that most of the changes occurred in distinct regions for the two stable groups. When a region exhibited significant changes in one stable group, it did not show changes in the other group. Thus, in these cases, the value of the change per month for the parameters with significant changes was similar to the difference between the monthly change in one group with respect to the other.

This study presents a series of limitations, including a restricted sample size reduced from 114 to 81 participants throughout the follow-up period. This limitation resulted in a reduction in statistical power, which is likely to have contributed to the scarcity of statistically significant results after correction for multiple comparisons. Moreover, no longitudinal data from healthy controls were available, and the assessment of the transition from EM to CM was not conducted due to the low sample size (two patients) related to the low annual incidence of this scenario (2.5–3.1%) and the use of preventive treatments after the first MRI acquisition. Consequently, the present study lacks quantification regarding the magnitude of change compared to baseline changes against controls, and of the transition from EM to CM.

An additional noteworthy limitation is the heterogeneity in preventive treatments. During the follow-up period, some patients with CM used two or more preventive treatments. The range of treatments varied widely, with most having very small sample sizes, except for topiramate. Thus, the use of multiple and diverse preventive treatments could potentially influence the results, although baseline comparisons exhibited similar patterns to the results at the longitudinal timepoint. Separately, in the patients with stable EM, we conducted an additional assessment including only the patients who used at least one preventive treatment. We observed additional significant changes, which might suggest specific effects related to preventive treatments.

Regarding the initial MRI acquisition, it is possible that the patients were in a preictal rather than an interictal stage, given that only the

**TABLE 6** The annual relative coefficient of the statistically significant (uncorrected $p < 0.05$) variations of the diffusion descriptors in all white matter regions based on the longitudinal coefficient of the complete generalized linear mixed model. Regions of interest were defined by the Johns Hopkins University ICBM-DTI-81 White Matter Atlas.

| | $EM_0 \rightarrow EM_1$ | | | $CM_0 \rightarrow EM_1$ | | | $CM_0 \rightarrow CM_1$ | | |
|---|---|---|---|---|---|---|---|---|---|
| **ROI** | **FA, %** | **AD, %** | **MD, %** | **FA, %** | **AD, %** | **MD, %** | **FA, %** | **AD, %** | **MD, %** |
| FOR | | | | | −0.34<br>$p = 0.034$ | | | | |
| L. CST | | | | 0.14<br>$p = 0.048$ | | | | | |
| L. ML | 0.20<br>$p = 0.013$ | | | | | | | | |
| L. SCP | | | | −0.14<br>$p = 0.043$ | | | | | |
| R. CP | **0.24***<br>**$p < 0.001$** | | | | | | 0.25<br>$p = 0.011$ | | |
| L. CP | 0.16<br>$p = 0.006$ | 0.23<br>$p = 0.015$ | | | | | 0.21<br>$p = 0.014$ | | |
| R. ALIC | | | | −0.17<br>$p = 0.022$ | | | | | |
| L. ALIC | | | | −0.12<br>$p = 0.040$ | | | | | |
| R. PLIC | 0.15<br>$p = 0.010$ | 0.21<br>$p = 0.018$ | | | | | | | |
| L. PLIC | | 0.22<br>$p = 0.020$ | | | | | | | |
| L. SCR | | | | −0.09<br>$p = 0.031$ | | | | | |
| L. UF | −0.31<br>$p = 0.006$ | | | | | | 0.26<br>$p = 0.013$ | | |
| R. TAP | | | | | | | 0.44<br>$p = 0.027$ | | |
| L. TAP | | | | | | | 0.47<br>$p = 0.043$ | | |

*Note*: The ROIs in bold represent large regions (volume >2000 $mm^3$). Cells in bold represent adjusted $p < 0.05$. All $p$ values are uncorrected.
Abbreviations: AD, axial diffusivity; ALIC, anterior limb of the internal capsule; $CM_0$, chronic migraine at baseline-time 0; $CM_1$, chronic migraine at longitudinal measurement-time 1; CP, cerebral peduncle; CST, corticospinal tract; $EM_0$, episodic migraine at baseline-time 0; $EM_1$, episodic migraine at longitudinal measurement-time 1; FA, fractional anisotropy; FOR, fornix; L., Left; MD, mean diffusivity; ML, medial lemniscus; PLIC, posterior limb of the internal capsule; R., right; ROI, region of interest; SCP, superior cerebellar peduncle; SCR, superior corona radiata; TAP, tapetum; UF, uncinate fasciculus.

preceding 24 h was considered in relation to headache and migraine attacks. This may introduce a degree of bias into the results. However, the subsequent 24 h was considered in the second MRI acquisition.

While these limitations exist, the study provides valuable insights, and a detailed examination of these constraints enhances the interpretation of its findings.

## CONCLUSIONS

We examined the structural changes in the brain of patients with migraine in relation to their clinical progression using longitudinal MRI data. The age-corrected results demonstrated significant longitudinal changes in all groups, predominantly in the GM and, to a lesser extent, in the WM. Patients with a stable diagnosis exhibited a greater number of longitudinal changes than those who improved from CM to EM, suggesting that clinical improvement does not result in significant brain structural changes. Conversely, the persistence of the condition does induce substantial alterations, particularly in regions associated with pain processing. These findings suggest that the brain adapts differently to stable and changing clinical conditions.

### AUTHOR CONTRIBUTIONS

**Álvaro Planchuelo-Gómez:** Conceptualization; data curation; formal analysis; investigation; methodology; software; supervision; validation; visualization; writing – original draft; writing – review and editing. **Carmen Martín-Martín:** Formal analysis; investigation; methodology;

software; visualization; writing – review and editing. **Ángel L. Guerrero:** Conceptualization; funding acquisition; investigation; project administration; resources; writing – review and editing. **David García-Azorín:** Conceptualization; investigation; project administration; resources; supervision; writing – original draft; writing – review and editing. **Rodrigo de Luis-García:** Conceptualization; funding acquisition; methodology; project administration; resources; writing – review and editing. **Santiago Aja-Fernández:** Conceptualization; funding acquisition; methodology; project administration; supervision; visualization; writing – original draft; writing – review and editing.

## ACKNOWLEDGMENTS

We like to acknowledge the Ethics Committee of Hospital Clínico Universitario de Valladolid and Laboratorio de Técnicas Instrumentales (Universidad de Valladolid).

## FUNDING INFORMATION

ThisstudywassupportedbygrantPID2021-124407NB-I00andTED2021-130758B-I00, funded by MCIN/AEI/10.13039/501100011033 and the European Union "NextGenerationEU/PRTR", being MCIN: Ministerio de Ciencia e Innovación (Spain); AEI: Agencia Estatal de Investigación (with DOI 10.13039/501100011033); and PRTR: Plan de Recuperación, Transformación y Resiliencia. There was further support by grant GRS 1727/A/18 from Gerencia Regional de Salud CyL. This work was funded by the Junta de Castilla y León and Fondo Social Europeo Plus (FSE+) under research grant VA156P24. ÁP-G was funded by the European Union-NextGenerationEU.

## CONFLICT OF INTEREST STATEMENT

**Álvaro Planchuelo-Gómez**, **Carmen Martín-Martín**, **Ángel L. Guerrero**, **David García-Azorín**, **Rodrigo de Luis-García**, and **Santiago Aja-Fernández** declare no conflicts of interest.

## ORCID

*Álvaro Planchuelo-Gómez* https://orcid.org/0000-0002-2188-4197

## REFERENCES

1. Ashina M, Terwindt GM, Al-Karagholi MAM, et al. Migraine: disease characterisation, biomarkers, and precision medicine. *Lancet*. 2021;397(10283):1496-1504. doi:10.1016/S0140-6736(20)32162-0
2. Demartini C, Francavilla M, Zanaboni AM, et al. Biomarkers of migraine: an integrated evaluation of preclinical and clinical findings. *Int J Mol Sci*. 2023;24(6):5334. doi:10.3390/ijms24065334
3. Jia Z, Yu S. Grey matter alterations in migraine: a systematic review and meta-analysis. *Neuroimage Clin*. 2017;14:130-140. doi:10.1016/j.nicl.2017.01.019
4. Rahimi R, Dolatshahi M, Abbasi-Feijani F, et al. Microstructural white matter alterations associated with migraine headaches: a systematic review of diffusion tensor imaging studies. *Brain Imaging Behav*. 2022;16(5):2375-2401. doi:10.1007/s11682-022-00690-1
5. Planchuelo-Gómez Á, García-Azorín D, Guerrero ÁL, Rodríguez M, Aja-Fernández S, de Luis-García R. Grey matter structural alterations in chronic and episodic migraine: a morphometric magnetic resonance imaging study. *Pain Med*. 2020;21(11):2997-3011. doi:10.1093/pm/pnaa271
6. Martín-Martín C, Planchuelo-Gómez Á, Guerrero ÁL, et al. Viability of AMURA biomarkers from single-shell diffusion MRI in clinical studies. *Front Neurosci*. 2023;17:1106350. doi:10.3389/fnins.2023.1106350
7. Planchuelo-Gómez Á, García-Azorín D, Guerrero ÁL, Aja-Fernández S, Rodríguez M, De Luis-García R. White matter changes in chronic and episodic migraine: a diffusion tensor imaging study. *J Headache Pain*. 2020;21(1):1. doi:10.1186/s10194-019-1071-3
8. Liu J, Lan L, Li G, et al. Migraine-related gray matter and white matter changes at a 1-year follow-up evaluation. *J Pain*. 2013;14(12):1703-1708. doi:10.1016/j.jpain.2013.08.013
9. Messina R, Rocca MA, Colombo B, et al. Gray matter volume modifications in migraine: a cross-sectional and longitudinal study. *Neurology*. 2018;91(3):e280-e292. doi:10.1212/WNL.0000000000005819
10. Lipton RB, Silberstein SD. Episodic and chronic migraine headache: breaking down barriers to optimal treatment and prevention. *Headache*. 2015;55(S2):103-122. doi:10.1111/head.12505_2
11. Wang SJ, Wu JW. Reversion from chronic migraine to episodic migraine: a new outcome measure. *Cephalalgia*. 2021;41(1):3-5. doi:10.1177/0333102420974004
12. Manack AN, Buse DC, Lipton RB. Chronic migraine: epidemiology and disease burden. *Curr Pain Headache Rep*. 2011;15(1):70-78. doi:10.1007/s11916-010-0157-z
13. Scher AI, Buse DC, Fanning KM, et al. Comorbid pain and migraine chronicity. *Neurology*. 2017;89(5):461-468. doi:10.1212/WNL.0000000000004177
14. Headache Classification Committee of the International Headache Society. The International Classification of Headache Disorders, 3rd edition. *Cephalalgia*. 2018;38(1):1-211. doi:10.1177/0333102413485658
15. Zigmond AS, Snaith RP. The hospital anxiety and depression scale. *Acta Psychiatr Scand*. 1983;67(6):361-370. doi:10.1111/j.1600-0447.1983.tb09716.x
16. Torres-Ferrús M, Quintana M, Fernandez-Morales J, Alvarez-Sabin J, Pozo-Rosich P. When does chronic migraine strike? A clinical comparison of migraine according to the headache days suffered per month. *Cephalalgia*. 2017;37(2):104-113. doi:10.1177/0333102416636055
17. Chalmer MA, Hansen TF, Lebedeva ER, Dodick DW, Lipton RB, Olesen J. Proposed new diagnostic criteria for chronic migraine. *Cephalalgia*. 2020;40(4):399-406. doi:10.1177/0333102419877171
18. Veraart J, Novikov DS, Christiaens D, Ades-Aron B, Sijbers J, Fieremans E. Denoising of diffusion MRI using random matrix theory. *NeuroImage*. 2016;142:394-406. doi:10.1016/j.neuroimage.2016.08.016
19. Cordero-Grande L, Christiaens D, Hutter J, Price AN, Hajnal JV. Complex diffusion-weighted image estimation via matrix recovery under general noise models. *NeuroImage*. 2019;200:391-404. doi:10.1016/j.neuroimage.2019.06.039
20. Kellner E, Dhital B, Kiselev VG, Reisert M. Gibbs-ringing artifact removal based on local subvoxel-shifts. *Magn Reson Med*. 2016;76(5):1574-1581. doi:10.1002/mrm.26054
21. Bautista T, O'Muircheartaigh J, Hajnal JV, Tournier JD. Removal of gibbs ringing artefacts for 3D acquisitions using subvoxel shifts. *2021 ISMRM Annual Meeting*; 2021:3535.
22. Tournier JD, Smith R, Raffelt D, et al. MRtrix3: a fast, flexible and open software framework for medical image processing and visualisation. *NeuroImage*. 2019;202:116137. doi:10.1016/j.neuroimage.2019.116137
23. Andersson JL, Sotiropoulos SN. An integrated approach to correction for off-resonance effects and subject movement in diffusion MR imaging. *NeuroImage*. 2016;125:1063-1078. doi:10.1016/j.neuroimage.2015.10.019
24. Smith SM, Jenkinson M, Woolrich MW, et al. Advances in functional and structural MR image analysis and implementation

as FSL. *NeuroImage*. 2004;23:S208-S219. doi:10.1016/j.neuroimage.2004.07.051
25. Zhang Y, Brady M, Smith S. Segmentation of brain MR images through a hidden Markov random field model and the expectation-maximization algorithm. *IEEE Trans Med Imaging*. 2001;20:45-57. doi:10.1109/42.906424
26. Dhollander T, Raffelt D, Connelly A. Unsupervised 3-tissue response function estimation from single-shell or multi-shell diffusion MR data without a co-registered T1 image. *ISMRM Workshop on Breaking the Barriers of Diffusion MRI*; 2016:5.
27. Jenkinson M, Beckmann CF, Behrens TE, Woolrich MW, Smith SM. FSL. *NeuroImage*. 2012;62:782-790. doi:10.1016/j.neuroimage.2011.09.015
28. Oishi K, Zilles K, Amunts K, et al. Human brain white matter atlas: identification and assignment of common anatomical structures in superficial white matter. *NeuroImage*. 2008;43(3):447-457. doi:10.1016/j.neuroimage.2008.07.009
29. Smith SM, Jenkinson M, Johansen-Berg H, et al. Tract-based spatial statistics: voxelwise analysis of multi-subject diffusion data. *NeuroImage*. 2006;31(4):1487-1505. doi:10.1016/j.neuroimage.2006.02.024
30. Dale AM, Fischl B, Sereno MI. Cortical surface-based analysis. I. Segmentation and surface reconstruction. *NeuroImage*. 1999;9(2):179-194. doi:10.1006/nimg.1998.0395
31. Fischl B, Liu A, Dale AM. Automated manifold surgery: constructing geometrically accurate and topologically correct models of the human cerebral cortex. *IEEE Trans Med Imaging*. 2001;20(1):70-80. doi:10.1109/42.906426
32. Fischl B, Salat DH, Busa E, et al. Whole brain segmentation: automated labeling of neuroanatomical structures in the human brain. *Neuron*. 2002;33(3):341-355. doi:10.1016/s0896-6273(02)00569-x
33. Ségonne F, Dale AM, Busa E, et al. A hybrid approach to the skull stripping problem in MRI. *NeuroImage*. 2004;22(3):1060-1075. doi:10.1016/j.neuroimage.2004.03.032
34. Desikan RS, Ségonne F, Fischl B, et al. An automated labeling system for subdividing the human cerebral cortex on MRI scans into gyral based regions of interest. *NeuroImage*. 2006;31(3):968-980. doi:10.1016/j.neuroimage.2006.01.021
35. Benjamini Y, Hochberg Y. Controlling the false discovery rate: a practical and powerful approach to multiple testing. *J R Stat Soc Ser B Methodol*. 1995;57(1):289-300. doi:10.2307/2346101
36. R Core Team. *R: A Language and Environment for Statistical Computing*; 2021. https://www.R-project.org/
37. Benarroch EE. What is the role of the cingulate cortex in pain? *Neurology*. 2020;95(16):729-732. doi:10.1212/WNL.0000000000010712
38. Zhang J, Su J, Wang M, et al. Increased default mode network connectivity and increased regional homogeneity in migraineurs without aura. *J Headache Pain*. 2016;17(1):98. doi:10.1186/s10194-016-0692-z
39. Mayr A, Jahn P, Stankewitz A, et al. Patients with chronic pain exhibit individually unique cortical signatures of pain encoding. *Hum Brain Mapp*. 2022;43(5):1676-1693. doi:10.1002/hbm.25750
40. Amaral VCG, Tukamoto G, Kubo T, Luiz RR, Gasparetto E, Vincent MB. Migraine improvement correlates with posterior cingulate cortical thickness reduction. *Arq Neuropsiquiatr*. 2018;76(3):150-157. doi:10.1590/0004-282x20180004
41. Liu HY, Chou KH, Chen WT. Migraine and the hippocampus. *Curr Pain Headache Rep*. 2018;22(2):13. doi:10.1007/s11916-018-0668-6
42. Schwedt TJ, Chong CD. Correlations between brain cortical thickness and cutaneous pain thresholds are atypical in adults with migraine. *PLoS One*. 2014;9(6):e99791. doi:10.1371/journal.pone.0099791
43. Schwedt TJ, Berisha V, Chong CD. Temporal lobe cortical thickness correlations differentiate the migraine brain from the healthy brain. *PLoS One*. 2015;10(2):e0116687. doi:10.1371/journal.pone.0116687
44. Chen ZH, Cui YL, Sun JT, et al. The brain structure and function abnormalities of migraineurs: a systematic review and neuroimaging meta-analysis. *Front Neurol*. 2022;13:1022793. doi:10.3389/fneur.2022.1022793
45. Qin ZX, Su JJ, He XW, et al. Altered resting-state functional connectivity between subregions in the thalamus and cortex in migraine without aura. *Eur J Neurol*. 2020;27(11):2233-2241. doi:10.1111/ene.14411
46. Lieberman G, Shpaner M, Watts R, et al. White matter involvement in chronic musculoskeletal pain. *J Pain*. 2014;15(11):1110-1119. doi:10.1016/J.JPAIN.2014.08.002
47. Yoon EJ, Kim YK, Shin HI, Lee Y, Kim SE. Cortical and white matter alterations in patients with neuropathic pain after spinal cord injury. *Brain Res*. 2013;1540:64-73. doi:10.1016/J.BRAINRES.2013.10.007
48. Liu J, Zhu J, Yuan F, Zhang X, Zhang Q. Abnormal brain white matter in patients with right trigeminal neuralgia: a diffusion tensor imaging study. *J Headache Pain*. 2018;19(1):46. doi:10.1186/s10194-018-0871-1
49. Yu D, Yuan K, Zhao L, et al. White matter integrity affected by depressive symptoms in migraine without aura: a tract-based spatial statistics study. *NMR Biomed*. 2013;26(9):1103-1112. doi:10.1002/nbm.2924
50. Planchuelo-Gómez Á, García-Azorín D, Guerrero ÁL, Rodríguez M, Aja-Fernández S, de Luis-García R. Structural brain changes in patients with persistent headache after COVID-19 resolution. *J Neurol*. 2023;170(1):13-31. doi:10.1007/s00415-022-11398-z

## SUPPORTING INFORMATION

Additional supporting information can be found online in the Supporting Information section at the end of this article.

**How to cite this article:** Planchuelo-Gómez Á, Martín-Martín C, Guerrero ÁL, García-Azorín D, de Luis-García R, Aja-Fernández S. Long-term evolution of white and gray matter structural properties in migraine. *Headache*. 2025;00:1-15. doi:10.1111/head.14949